Anisotropy models for spatial data

Denis Allard, Rachid Senoussi, Emilio Porcu

Math Geosci
DOI 10.1007/s11004-015-9594-x

SPECIAL ISSUE

Anisotropy Models for Spatial Data

D. Allard[1] · **R. Senoussi**[1] · **E. Porcu**[2]

Received: 24 September 2014 / Accepted: 26 March 2015

Abstract This work addresses the question of building useful and valid models of anisotropic variograms for spatial data that go beyond classical anisotropy models, such as the geometric and zonal ones. Using the concept of principal irregular term, variograms are considered, in a quite general setting, having regularity and scale parameters that can potentially vary with the direction. It is shown that if the regularity parameter is a continuous function of the direction, it must necessarily be constant. Instead, the scale parameter can vary in a continuous or discontinuous fashion with the direction. A directional mixture representation for anisotropies is derived, in order to build a very large class of models that allow to go beyond classical anisotropies. A turning band algorithm for the simulation of Gaussian anisotropic processes, obtained from the mixture representation, is then presented and illustrated.

Keywords Anisotropy · Covariance · Isotropy · Spatial statistics · Turning band method · Variogram

1 Introduction

In spatial statistics the assumption of isotropy is very common despite being very restrictive for describing the rich variety of interactions that can characterize spatial

✉ D. Allard
allard@avignon.inra.fr

E. Porcu
porcu@usm.cl

[1] UR546 Biostatistique et Processus Spatiaux (BioSP), 84914 Avignon, France

[2] Departamento de Matematica, Universidad Santa Maria, Valparaiso, Chile

Published online: 08 April 2015

processes. This is probably due to a combination of at least two reasons. Isotropic models are obviously mathematically easier to build than anisotropic ones and, being more parsimonious, the estimation of their parameters is more feasible, in particular when the sample size is small. When anisotropy is modeled, anisotropic models are in the vast majority of cases restricted to the classical geometric and zonal anisotropy models, which in essence amounts to transform the coordinates by means of a transformation matrix (Chilès and Delfiner 2012). The literature on anisotropy models evading from these two classical models is very sparse, at the exception of the approaches based on componentwise anisotropy (Ma 2007; Porcu et al. 2006).

The present work has been prompted by the following question, not uncommon in geostatistics. Suppose that, when exploring a given spatial dataset, the empirical variograms computed in different directions show not only varying ranges and/or sills, but also significantly different behaviors at the origin, for example close to a quadratic behavior in one direction and close to a linear behavior in the perpendicular direction. It is well known that the presence of a linear trend in one direction induces a quadratic behavior of the empirical variogram along that direction. The scientist modeling such data is thus faced with the following problem: should these variations of regularity be modeled by adding a linear trend, or can they be modeled within the random field model using a variogram model whose regularity parameter changes with the direction as proposed in Eriksson and Siska (2000) and Dowd and Igúzquiza (2012)? Providing a definitive answer to this question requires to first address a collection of theoretical issues. Is such a model admissible? Can we find necessary and sufficient validity conditions for anisotropy models? Can we find a full characterization of admissible anisotropy models, having zonal and geometrical models as special cases? Can we easily simulate from those?

The purpose of this paper is to provide a full characterization of admissible anisotropy models and, based on this, to propose a large class of anisotropy models that includes all known models of anisotropy. Section 2 sets the notations and makes general reminders on variograms that will be useful for the presentation of our findings. In particular, spectral representation and characterization of the regularity at the origin by means of the principal irregular term are recalled. In Sect. 3 the usual anisotropy models are reviewed. Section 4 is the theoretical core of our work. From a result on fractal dimensions of surface roughness in Davies and Hall (1999), it is shown that when the regularity of a variogram in $\mathbb{R}^d$ varies continuously with the direction, it must be equal to a given constant in all directions. As a consequence, on the plane, the regularity parameter of a variogram must be the same in all directions, with the exception of one single direction where it can be larger than the common value. Then, a full characterization of admissible anisotropies is obtained, based on a result in Matheron (1975). This result is revisited, and its equivalence with directional mixtures of zonal anisotropies is shown. Through parametric or non-parametric constructions, it allows to evade from the classical anisotropy models and it provides the basis for simulating anisotropic random fields using a modified turning band algorithm. New anisotropy models are presented on the plane, along with realizations from these models.

2 Covariance Functions and Variograms

2.1 Stationarity and Spectral Representations

Second-order properties of Gaussian fields which are necessary for the rest of this paper are briefly recalled. This part is largely expository and the reader is referred to Chilès and Delfiner (2012), Gneiting et al. (2001), and the more recent paper by Porcu and Schilling (2011) for a thorough overview. Gaussian fields, that are either second-order or intrinsically stationary, will be denoted $\{Z(s)\}$, $s \in \mathbb{R}^d$. The former assumes that the first-order moment is finite and constant, and that the covariance $\text{cov}\{Z(s), Z(s')\}$ depends exclusively on the lag vector $s - s'$, thus defining the covariance function $C : \mathbb{R}^d \to \mathbb{R}$

$$C(h) = \text{cov}\{Z(s), Z(s+h)\}, \quad s, h \in \mathbb{R}^d.$$

The assumption of intrinsic stationarity is more relaxed. A Gaussian field is called intrinsically stationary if first and second moments of differences $Z(s+h) - Z(s)$ are finite and stationary, thus defining the variogram $\gamma : \mathbb{R}^d \to \mathbb{R}^+$

$$\gamma(h) = 0.5\text{var}\{Z(s+h) - Z(s)\} = 0.5E[\{Z(s+h) - Z(s)\}^2], \quad s, h, \in \mathbb{R}^d.$$

For the remainder of the paper, it will be useful to decompose the vector $h = (h_1, \ldots, h_d) \in \mathbb{R}^d$ into its modulus $r = \|h\|$ and its direction $\theta \in \mathbb{S}^{d-1}$, thus writing $h = (r, \theta) \in \mathbb{R}^+ \times \mathbb{S}^{d-1}$. The Euclidean norm of h will be indifferently denoted r or $\|h\|$, depending on the context. For two directions θ and η belonging to $\mathbb{S}^{d-1}$, with a slight abuse of notations, we will write $\cos(\eta - \theta) = \cos(\eta, \theta) =< \eta, \theta >$, since $\|\eta\| = \|\theta\| = 1$.

Parameters of covariance functions relate in general to variance, scale and regularity at the origin. Unbounded variograms are associated to intrinsic random functions for which the variance of $Z(\cdot)$ is infinite. For bounded variograms, it is well known that the sill of the variogram, σ^2, must be identical in all direction. Without loss of generality, $\sigma^2 = 1$ from now on, except if explicitly stated otherwise. Discontinuities at the origin of the variogram do not depend on direction. Thus, only variograms continuous at the origin will be considered from now on. The scale parameter, denoted b, is associated to the lag vector h or its modulus $\|h\|$. In our notations, b is homogeneous to $\|h\|$, so that covariance functions and variograms will be functions of the ratio h/b.

A necessary and sufficient condition for a candidate mapping $C : \mathbb{R}^d \to \mathbb{R}$ to be a covariance function is that of positive definiteness: for any finite dimensional collection of points $\{s_i\}_{i=1}^n$ and any real coefficients $\{a_i\}_{i=1}^n$, the condition $\sum_{i=1}^n \sum_{j=1}^n a_i C(s_i - s_j) a_j \geq 0$ is verified. The function C is characterized through Bochner's theorem as being the Fourier transform of a positive and bounded measure.

A necessary and sufficient condition for $\gamma : \mathbb{R}^d \to \mathbb{R}$ to be a variogram is that of conditional negative definiteness, that is, the inequality above reads: $-\sum_{i=1}^n \sum_{j=1}^n a_i \gamma(s_i - s_j) a_j \geq 0$, the coefficients $\{a_i\}_{i=1}^n$ being additionally restricted to be a contrast, that is $\sum_{i=1}^n a_i = 0$. The class of variograms being broader than that of covariance functions, more attention will be given through the manuscript

to variograms rather than covariances. The set of variograms is a convex cone, closed under pointwise convergence and linear combinations with non-negative coefficients. As a result, mixtures of variograms $\gamma(\cdot;\xi)$ with respect to non negative, finite, mixtures $\mu(\mathrm{d}\xi)$ are variograms. The analogue of Bochner's representation theorem for variograms is due to Schoenberg (1938), Chilès and Delfiner (2012).

Theorem 1 (Schoenberg 1938) *Let $\gamma : \mathbb{R}^d \to \mathbb{R}$ be a continuous function satisfying $\gamma(0) = 0$. The following three properties are equivalent*

(i) *$\gamma(\cdot)$ is a variogram on $\mathbb{R}^d$;*
(ii) *$\exp\{-\xi\gamma(\cdot)\}$ is a covariance function for all $\xi > 0$;*
(iii) *$\gamma(\cdot)$ is of the form*

$$\gamma(h) = \int_{\mathbb{R}^d} \frac{1 - \cos(2\pi < \omega, h >)}{4\pi^2\|\omega\|^2} \chi(\mathrm{d}\omega), \tag{1}$$

where χ is a positive symmetric measure with no atom at the origin and satisfying

$$\int_{\mathbb{R}^d} \frac{\chi(\mathrm{d}\omega)}{1 + 4\pi^2\|\omega\|^2} < \infty. \tag{2}$$

The spectral measure of the variogram is $\nu(\mathrm{d}\omega) = \chi(\mathrm{d}\omega)/4\pi^2\|\omega\|^2$. The condition in Eq. (2) is equivalent to $\int_{\|\omega\|\geq\varepsilon} \nu(\mathrm{d}\omega) < \infty$ and $\int_{\|\omega\|<\varepsilon} \|\omega\|^2\nu(\mathrm{d}\omega) < \infty$, for all $\varepsilon > 0$. As a direct application of Theorem 1, the function $\gamma(h) = c\|h\|^\beta$ is a valid variogram for $0 < \beta < 2$ and $c > 0$ in $\mathbb{R}^d$, for any $d \in \mathbb{N}$. It is referred to as the "power variogram". Its associated measure $\chi(\mathrm{d}\omega)$ is proportional to $\|\omega\|^{2-\beta-d}\mathrm{d}\omega$. If $\nu(\mathbb{R}^d) < \infty$, $\gamma(\cdot)$ is of the form $\sigma^2\{1 - \int_{\mathbb{R}^d} \cos(2\pi < \omega, h >)\nu(\mathrm{d}\omega)\}$. In this case the variogram is bounded and there exists a covariance function $C : \mathbb{R}^d \to \mathbb{R}$, with spectral measure ν as above, such that $\gamma(h) = C(0) - C(h)$.

2.2 Mixture Representation of Isotropic Covariance Functions and Variograms

Covariance functions and variograms are called isotropic or radially symmetric when there exists mappings $\varphi : [0, \infty) \to \mathbb{R}$ and and $\psi : [0, \infty) \to \mathbb{R}^+$ such that

$$C(h) = \varphi(\|h\|), \quad \gamma(h) = \psi(\|h\|), \quad h \in \mathbb{R}^d.$$

Following Daley and Porcu (2014), Φ_d denotes the class of continuous mappings $\varphi : [0, \infty) \to \mathbb{R}$ with $\varphi(0) = 1$ and such that there exists a weakly stationary Gaussian field on $\mathbb{R}^d$ whose covariance function is $\varphi(\|h\|)$. The classes Φ_d are nested, so that $\Phi_1 \supset \Phi_2 \supset \cdots \supset \Phi_\infty = \bigcap_{k\geq 1} \Phi_k$, the inclusion relation being strict, where Φ_∞ is the class of functions which are isotropic and positive definite on any d-dimensional Euclidean space. Analogously, the class Ψ_d is the set continuous mappings $\psi : [0, \infty) \to \mathbb{R}^+$ such that there exists a weakly or an intrinsically stationary Gaussian field whose variogram is $\psi(\|h\|)$. The class Ψ_d is also strictly nested. If $Z(\cdot)$ is weakly stationary with covariance function $\varphi \in \Phi_d$, the function ψ such that

Table 1 Some unbounded elements of the class Ψ_∞

Variogram	Name	Parameters
$\psi(r) = (r/b)^\beta$	Power	$0 < \beta \leq 2,\ b > 0$
$\psi(r) = [(r/b)^\beta + 1]^\alpha - 1$	Gen. power	$0 < \beta \leq 2,\ 0 < \alpha < 1,\ b > 0$
$\psi(r) = \log[(r/b)^\beta + c] - \log c$	Log-power	$0 < \beta \leq 2,\ b > 0,\ c > 1.$

$\psi(\cdot) = \varphi(0) - \varphi(\cdot)$ belongs necessarily to Ψ_d. There are however functions of Ψ_d without counterpart in Φ_d. Table 1 provides examples of unbounded members of Ψ_∞.

A mapping γ from $\mathbb{R}^d$ to $\mathbb{R}$ is said to be the radial or isotropic version of a member of the class Ψ_d when $\gamma(h) = \psi(\|h\|)$. Anisotropic covariance functions will be derived by applying to $\psi \in \Psi_d$ a scaling factor $b(\theta)$ function of the direction $\theta = h/\|h\|$, that is $\gamma(h) = \psi\{\|h\|/b(\theta)\}$.

2.3 Regularity and Principal Irregular Term within the Class Ψ_d

Regularity properties are presented under the assumption of isotropy. Characterization of the regularity of anisotropic variograms is fully addressed in Sect. 4. The behavior of the variogram near the origin is one of its most important characteristics. It relates to the regularity of the associated random field and infill asymptotic properties (Stein 1999). Mean squared continuity of the random field is equivalent to the variogram being continuous at the origin. A variogram that is $2m$ times differentiable at the origin corresponds to a random field that is m times mean squared differentiable.

The regularity properties of isotropic variograms on $\mathbb{R}^d$ is given by the behavior of $\psi \in \Psi_d$ as $r \to 0^+$. All functions in Table 1 behave as $a(r/b)^\beta + o(r^\beta)$ when $r \to 0^+$, with $0 < \beta \leq 2$ and $a > 0$, so that the correspondent radial version γ will behave as $a(\|h\|/b)^\beta + o(r^\beta)$, as $\|h\| \to 0$. Similar observations can be made for members of the class Φ_d. In this class, regularity properties are characterized by the behavior of $1 - \varphi(r)$ as $r \to 0^+$ which, with a slight abuse of language, will be referred to as the regularity at the origin or the behavior at the origin of the covariance function. For instance, the powered exponential covariance $C(r) = \exp\{-(r/b)^\beta\}$ and the Cauchy covariance $C(r) = \{1 + (r/b)^\beta\}^{-\alpha/\beta}$, with $0 < \beta \leq 2$, $\alpha > 0$ and $b > 0$ also behave as $1 - c(r/b)^\beta + o(r^\beta)$ when $r \to 0^+$. The behavior at the origin of the Matérn covariance function

$$C_{\mathrm{Mat}}(r) = \frac{1}{2^{\kappa-1}\Gamma(\kappa)} \left(\frac{r}{b}\right)^\kappa K_\kappa \left(\frac{r}{b}\right), \quad r \in [0, \infty),$$

where $b, \kappa > 0$, depends on the parameter κ. It is proportional to $(r/b)^{2\kappa}$ if $0 < \kappa < 1$; it is proportional to $(r/b)^2 \log(r/b)$ if $k = 1$ and proportional $(r/b)^2$ whenever $\kappa \geq 1$.

Following Stein (1999) the regularity of an isotropic variogram is described using the concept of principal irregular term which relates to the property of $\psi(r)$ when $\psi \in \Psi_d$ and r tends to zero from above. Loosely speaking, the principal irregular term is the term r^β with lowest degree of the series expansion of $\psi(r)$ that is not an even power (Chilès and Delfiner 2012; Matheron 1970). Stein (1999) defines the principal irregular

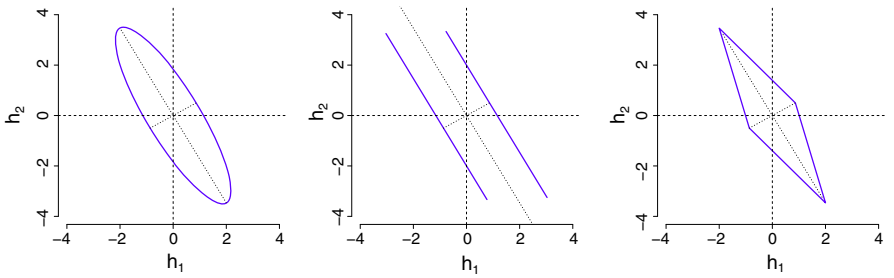

Fig. 1 Examples of geometric (*left*), zonal (*center*) and separable anisotropy (*right*). Each *panel* shows in a polar representation the graph of the scale parameter $b(\theta)$ as a function of the angle θ, for $b_1 = 1, b_2 = 4$ and $\theta_0 = \pi/6$ for an exponential variogram (i.e. $\beta = 1$)

term of $\psi(r)$ as the function g such that $g(r)r^{-2n} \to 0$ and $|g(r)|r^{-2n-2} \to \infty$ for some $n \geq 0$ as $r \to 0^+$ and $\gamma(r) = \sum_{j=0}^{n} c_j r^{2j} + g(r) + o(|g(r)|)$ as $r \to 0^+$. On the examples seen so far and for virtually all models used in practice, principal irregular terms are either of the form $g(r) = \alpha r^{\beta}$, for $0 < \beta < 2$, or $g(r) = \alpha r^{2k} \log r$, for some positive integer k. Obviously, for power variograms, it is the power variogram itself.

3 Overview of Anisotropy Models

Anisotropy is usually modeled through geometric, zonal or separable models of anisotropy. These elementary models of anisotropy can be composed to provide more complex anisotropies, as in Journel and Froidevaux (1982).These models are briefly recalled, before being extended in a common framework in Sect. 4. They are illustrated on the plane in Fig. 1.

3.1 Geometric Anisotropy

A variogram in $\mathbb{R}^d$ displays a geometric anisotropy if it is of the form $\gamma(h) = \psi(\|Ah\|)$, for $\psi \in \Psi_d$, where A is the product between a diagonal matrix of scaling factors, say D, and a rotation matrix (Chilès and Delfiner 2012). The function γ inherits the properties of the associated $\psi \in \Psi_d$ in terms of regularity in all directions. It can be shown that the contour lines of this variogram are represented by ellipsoids. If $\psi(r) = r$, the inverse of the slope of $\gamma(h)$ as a function of the direction θ is represented by an ellipsoid. Figure 1 (left panel) provides an illustration of a geometrical anisotropy in $\mathbb{R}^2$. It shows, in a polar representation, the graph of the scale parameter $b(\theta)$ of the exponential variogram

$$\begin{aligned}\gamma(h) &= 1 - \exp\{-r/b(\theta)\} \\ &= 1 - \exp\left[-r\left\{b_1^{-2}\cos^2(\theta-\theta_0) + b_2^{-2}\sin^2(\theta-\theta_0)\right\}^{1/2}\right],\end{aligned}$$

with $b(\theta) = \{b_1^{-2}\cos^2(\theta-\theta_0) + b_2^{-2}\sin^2(\theta-\theta_0)\}^{-1/2}$. As expected, the shape of the graph is an ellipse.

3.2 Zonal Anisotropy

Zonal anisotropy is a degenerate case of geometrical anisotropy, obtained when some of the diagonal elements of D are equal to 0. Suppose that the d' non null components of D are the d' first coordinates of $\mathbb{R}^d$. Then, the variogram is strictly equal to 0 in any direction perpendicular to $\mathbb{R}^{d'}$. Equivalently, the associated random field is constant within any subspace of $\mathbb{R}^d$ that is perpendicular to $\mathbb{R}^{d'}$. Of particular importance for the rest of this work will be the case $d' = 1$ for which the variogram depends only on one component. Fix $\theta_0 \in \mathbb{S}^{d-1}$. The corresponding zonal anisotropy variogram in a direction θ is then

$$\gamma(h) = \psi\{r|\cos(\theta - \theta_0)|\}, \tag{3}$$

where $\psi \in \Psi_d$. If ψ has sill σ^2 and range b, the variogram γ in a given direction θ has sill σ^2 and range $b/|\cos(\theta - \theta_0)|$, except in any direction perpendicular to θ_0 where the variogram is identically zero. Figure 1 (central panel) is an example of zonal anisotropy in the plane. It shows $b(\theta)$ as a function of θ for the exponential variogram

$$\gamma(h) = 1 - \exp\{-r/b(\theta)\} = 1 - \exp\{-r|\cos(\theta - \theta_0)|/b_1\},$$

where $b(\theta) = b_1/|\cos(\theta - \theta_0)|$. The graph is made of two parallel lines, which can be viewed as the degenerate case of an ellipse when the major axis tends to infinity.

In practice, a real phenomenon is rarely modeled through a pure zonal model. In general, there are several components $\gamma_j(h)$ with $\gamma(h) = \sum_{j=1}^{J} \gamma_j(h)$, some of which being zonal. There is a large variety of possible situations, which will not be detailed here. Interested readers are referred to Chilès and Delfiner (2012) for illustrative examples. With zonal anisotropy, one can model variograms whose regularity varies with directions, as shown in the following example. In $\mathbb{R}^2$, let $\gamma(h) = \gamma_1(h) + \gamma_2(h)$, where $\gamma_1(h)$ has a zonal anisotropy with $\gamma_1(h) = (r|\cos\theta|)^{\beta_1}$ and $\gamma_2(h)$ is isotropic with $\gamma_2(h) = r^{\beta_2}$. Let further assume that $\beta_1 < \beta_2$. Then, along all directions $\theta \notin \{\pi/2, -\pi/2\}$ the principal irregular term is equal to r^{β_1}. For $\theta \in \{\pi/2, -\pi/2\}$, it is equal to r^{β_2}, which is more regular than r^{β_1}. In this example, the principal irregular term of the variogram varies with θ, but only discontinuously along the Y axis.

3.3 Separability: Componentwise Anisotropy

This case corresponds, possibly after appropriate rotation, to the tensorial product

$$C(h) = \prod_{i=1}^{p} C_i(h_i) = \prod_{i=1}^{p} \varphi_i(\|h_i\|), \quad \varphi_i \in \Phi_{d_i},$$

where $h_i \in \mathbb{R}^{d_i}$ and $\sum_{i=1}^{p} d_i = d$. These models are also called separable. The function C is the tensor product of the radial versions of members of the classes Φ_{d_i}, $i = 1, \ldots, p$. It is for example the covariance function of the random field $Z(s) = \prod_{i=1}^{p} Z_i(s_i)$, where $Z_i(s_i)$ is any random field with covariance C_i on $\mathbb{R}^{d_i}$, independent on all other random fields $Z_j(\cdot)$, $j \neq i$.

Table 2 Possible shapes of the graph of $b(\theta)$ for three classical models of anisotropy. The parameter β is the exponent of the principal irregular term

Model	$0 < \beta < 1$	$\beta = 1$	$1 < \beta < 2$	$\beta = 2$
Geometric	Ellipse	Ellipse	Ellipse	Ellipse
Zonal	Parallel lines	Parallel lines	Parallel lines	Parallel lines
Separable	4-cusp hypocycloïd	Rhombus	Convex	Ellipse

The parameter β is the exponent of the principal irregular term

Separable models can also lead to discontinuities of the regularity parameter with respect to the direction on a finite set of directions, as illustrated in the following example. Let us consider, in $\mathbb{R}^2$, the product of the two stable covariance functions $\exp\{-|h_1|^{\beta_1}\}$ and $\exp\{-|h_2|^{\beta_2}\}$, with $\beta_1 < \beta_2$. Then, the corresponding variogram is

$$\begin{aligned}\gamma(h) &= 1 - \exp\{-|h_1|^{\beta_1}\}\exp\{-|h_2|^{\beta_2}\} \\ &= 1 - \exp\{-r^{\beta_1}[|\cos\theta|^{\beta_1} + r^{\beta_2-\beta_1}|\sin\theta|^{\beta_2}]\},\end{aligned}$$

which shows that the principal irregular term is r^{β_1} in all directions $\theta \notin \{\pi/2, -\pi/2\}$, whereas it is r^{β_2} in the directions $\{\pi/2, -\pi/2\}$. The right panel in Fig. 1 represents the anisotropy of the following separable model of covariance

$$\gamma(h) = 1 - \exp\{-r/b(\theta)\} = 1 - \exp\{-rb_1^{-1}|\cos(\theta - \theta_0)| - rb_2^{-1}|\sin(\theta - \theta_0)|\},$$

with $b(\theta) = \{b_1^{-1}|\cos(\theta-\theta_0)|+b_2^{-1}|\sin(\theta-\theta_0)|\}^{-1}$. Notice that the same behavior of the principal irregular term was also obtained with a very different model of variogram in the previous paragraph.

The shapes of the graph of $b(\theta)$ obtained in Fig. 1 differ greatly with the type of anisotropy model. The possible shapes of the graph of $b(\theta)$ that can be obtained for these three classical models of anisotropy in the plane are summarized in Table 2. Geometric anisotropies yield always elliptical shapes, whereas graphs associated to zonal anisotropies are always the union of two parallel lines. For separable anisotropies the shape of the graph varies with β, from 4-cusp hypocycloïds when $0 < \beta < 1$ to ellipses when $\beta = 2$.

4 A General Characterization of Anisotropy

A complete characterization of anisotropic variograms is now provided. First is addressed the characterization of the regularity at the origin. It will be shown that regularity parameters that vary continuously with the direction must be constant. A complete characterization of the scale parameter is then provided.

4.1 Isotropy of the Regularity at the Origin

Eriksson and Siska (2000) and Dowd and Igúzquiza (2012) proposed the following anisotropic power variogram model in $\mathbb{R}^2$

$$\gamma_{\mathrm{AP}}(h) = a(\theta) r^{\beta(\theta)}, \quad h = (r, \theta) \in \mathbb{R}^+ \times [0, 2\pi),$$

in which the scale parameter $a(\theta)$ and the power coefficient $\beta(\theta)$ are continuous functions of θ, with the usual restriction $a(\theta) > 0$ and $0 < \beta(\theta) \leq 2$. The mapping $\beta(\cdot)$ relates to the regularity at the origin of the variogram, or equivalently to the smoothness of the random field (Stein 1999), whilst the function $a(\cdot)$ is a scaling factor. It was further proposed that $\beta(\theta)$ varies in a way similar to the geometric anisotropy, that is according to an ellipse.

The model $\gamma_{\mathrm{AP}}(h)$ is unfortunately not valid, except in a very particular case. In Davies and Hall (1999) it was shown that if a random field has a well defined fractal index in each direction, then the fractal dimensions of its line transect processes are the same in all directions, except possibly one, whose dimension may be less than in all others. For power variograms, the fractal dimension in direction θ, $D(\theta)$, is related to $\beta(\theta)$ through $D(\theta) = d + 1 - \frac{1}{2}\beta(\theta)$. As a direct application, a necessary condition for the above model to be valid is thus that $\beta(\cdot) = \beta$ in all directions, except one where it can be larger than β, which leads to the following proposition, adapted from Davies and Hall (1999).

Proposition 1 *The function γ_{AP}: $R^+ \times \mathbb{S}^{d-1} \to \mathbb{R}^+$ with $h = (r, \theta)$, $d \geq 2$ and such that $\gamma_{\mathrm{AP}}(h) = a(\theta) r^{\beta(\theta)}$, where $a(\theta) > 0$ and where $\beta(\theta)$ is a continuous function on $\mathbb{S}^{d-1}$ with $0 < \beta(\theta) \leq 2$, is a valid variogram on $\mathbb{R}^d$ if and only if $\beta(\theta)$ is constant on $\mathbb{S}^{d-1}$.*

The proof, shortly sketched here, will be used for the next Theorem. For the sake of completeness, it is provided in Appendix. The "if" part is straightforward, since the power variogram $\gamma(h) = a(\theta) r^{\beta}$ is valid on $\mathbb{R}^d$, $d \geq 1$, provided that $a(\theta)$ is a valid model of anisotropy. The "only if" part is proven by building a simple counter-example in $\mathbb{R}^2$. It is shown that the conditional definite negativeness condition is not verified for the contrast $Z(0,0) - Z(-r\cos\theta, r\sin\theta)/2 - Z(r\cos\theta, r\sin\theta)/2$ as $r \to 0$, unless $\beta(\theta)$ is constant. The proof is then completed by noticing that a function not c.d.n. in $\mathbb{R}^2$ is necessarily not c.d.n. in $\mathbb{R}^d$, for $d > 2$.

The next step is to make this statement more general, thus leading to our main theoretical result. It is expected that Proposition 1 holds for a much larger class of variograms than power variograms, as formally stated below. We first recall that a function $f : \mathbb{R}^+ \to \mathbb{R}^+$ is said to be regularly varying at 0 if $\lim_{r \to 0} f(\alpha r)/f(r) < \infty$ for all $\alpha > 0$. Polynomials, power functions and logarithms are regularly varying functions at 0.

Theorem 2 *Let $Z(\cdot)$ be an intrinsic random field on $\mathbb{R}^d$ with a continuous variogram $\gamma(\cdot)$ in the class Ψ_d with a behavior at the origin of the form*

$$g(h) = a(\theta) r^{\beta(\theta)} f(r), \tag{4}$$

where $0 < \beta(\cdot) \leq 2$, the function $a(\cdot)$ is a positive, finite, continuous function on $\mathbb{S}^{d-1}$ and the function $f(\cdot)$ is regularly varying. Then, if $\beta(\cdot)$ is a continuous function on $\mathbb{S}^{d-1}$, it is constant.

The proof of Theorem 2 is given in Appendix. Particular cases for condition (4) are $f(r) = 1$ and $f(r) = \log r$, which lead to principal irregular terms of the form $g_\theta(r) = r^{\beta(\theta)}$, respectively $g_\theta(r) = r^2 \log r$ when $\beta = 2$. Proposition 1 is thus a special case of Theorem 2. Conditions of Theorem 2 are quite general, since they include all known expressions of principal irregular terms. They are verified by virtually all variograms used in practice: Matérn class, Cauchy variograms, power variograms, logarithm variogram, etc.

Theorem 2 thus states very generally that the regularity of a variogram, and hence that of the associated random field cannot vary continuously with the direction. When the regularity parameter varies, it is only possible along some directions: in the plane, there is at most one direction corresponding to a zonal anisotropy model along which the regularity is smoother than in any other direction. In the three-dimensional space, there is either a single direction, or a single plane on which the regularity is smoother.

4.2 Anisotropy of the Scale Parameter as Directional Mixtures of Zonal Anisotropies

Let us first go back to variograms behaving near the origin according to

$$\gamma(h) = a(\theta) r^\beta + o(r^\beta), \quad h = (r, \theta) \in \mathbb{R}^+ \times \mathbb{S}^{d-1}, \tag{5}$$

with $0 < \beta \leq 2$. In order to define a valid model of variogram in $\mathbb{R}^d$, the function $a(\theta)$ has to verify some conditions. Necessary and sufficient conditions for $a(\theta)$ were presented in Matheron (1975). It is rephrased below, using our notations.

Theorem 3 (Matheron 1975) *Suppose γ is a variogram on $\mathbb{R}^d$ such that, for any direction $\theta \in \mathbb{S}^{d-1}$, Eq. (5) holds with $a : \mathbb{S}^{d-1} \to \mathbb{R}^+$ being a continuous mapping, and $0 < \beta < 2$. Then, as $\|h\| \to 0$, the variogram admits a representation (5) with*

$$a(\theta) = \int_{\mathbb{S}^{d-1}} |\cos(\theta - \eta)|^\beta \nu(\mathrm{d}\eta), \tag{6}$$

where ν is a uniquely determined finite, non negative, symmetric, measure on $\mathbb{S}^{d-1}$. Conversely, if the representation (6) exists, the function $\gamma(h)$ is a variogram.

Readers are referred to Matheron (1975) for the original proof. From Theorem 3, we are now able to provide a full characterization of the anisotropic variograms when $0 < \beta < 2$.

Theorem 4 *Suppose γ is a function such that, for any direction θ, Eq. (5) holds. Then, γ is a valid variogram in $\mathbb{R}^d$ if and only if it is a finite, non negative, directional mixture of zonal anisotropy versions of a radial variogram $\psi \in \Psi_d$*

$$\gamma(h) = \int_{\mathbb{S}^{d-1}} \psi(r|\cos(\theta - \eta)|)\nu(\mathrm{d}\eta), \tag{7}$$

where ν is a finite, non negative, mixture on $\mathbb{S}^{d-1}$.

Moreover, the scale parameter is

$$b(\theta) = \left\{ \int_{\mathbb{S}^{d-1}} |\cos(\theta - \eta)|^{\beta} \nu(\mathrm{d}\eta) \right\}^{-1/\beta}, \tag{8}$$

for some non negative, symmetric, measure ν defined on $\mathbb{S}^{d-1}$.

Proof The "if" part is straightforward. It follows from the fact that the class Ψ_d is a convex cone closed under pointwise convergence. The "only if part" is a consequence of Matheron's theorem, as shown now. Consider the function $\gamma(h) = \psi\{\|h\|/b(\theta)\}$, where $b(\theta)$ is a continuous function of $\theta \in \mathbb{S}^{d-1}$ and where $\psi(r) \sim ar^{\beta}$ as $r \to 0$, with $a > 0$. Then, Theorem 3 states that the function $\gamma(h) = \psi\{\|h\|/b(\theta)\}$ is a valid anisotropic variogram if and only if the scale parameter $b(\theta)$ varies with the direction according to Eq. (8), thus leading to variograms verifying Eq. (6) as $r \to 0$.

On the other hand, this representation actually corresponds to a directional mixture of zonal anisotropies, as defined in Eq. (3). Let $Y(z)$, $z \in \mathbb{R}$, be an intrinsic random function with radial variogram $\psi \in \Psi_d$ and let $\eta \in \mathbb{S}^{d-1}$ be a direction in $\mathbb{R}^d$. Let us define $Z_\eta(s)$ as the zonal anisotropic random field

$$Z_\eta(s) = Y\{\|s\| \cos(\eta - \|s\|^{-1}s)\}, \quad s \in \mathbb{R}^d.$$

The variogram of $Z_\eta(s)$ is thus

$$\gamma_\eta(h) = \psi\{r|\cos(\theta - \eta)|\}, \quad h \in \mathbb{R}^d.$$

Let us now consider that η is a random direction with probability measure $\tilde{\nu}(\cdot) = \nu(\cdot)/\nu([0, 2\pi[)$ on $\mathbb{S}^{d-1}$ and let us define the mixture random field

$$Z(s) = Z_\eta(s), \quad \eta \sim \tilde{\nu}.$$

Then, the variogram of $Z(\cdot)$ is

$$\begin{aligned}\gamma(h) &= 0.5E[\{Z(s) - Z(s+h)\}^2] = E_{\tilde{\nu}}[0.5E[\{Z_\eta(s) - Z_\eta(s+h)\}^2 \mid \eta]] \\ &= E_{\tilde{\nu}}[\gamma_\eta(h)] = \int_{\mathbb{S}^{d-1}} \psi(r|\cos(\theta - \eta)|)\tilde{\nu}(\mathrm{d}\eta).\end{aligned}$$

Since $\psi(r) \sim ar^{\beta}$ as $r \to 0$, we thus have

$$\gamma(h) = r^{\beta} \int_{\mathbb{S}^{d-1}} |\cos(\theta - \eta)|^{\beta} a\tilde{\nu}(\mathrm{d}\eta),$$

as $\|h\| \to 0$, which is equivalent to Eq. (6) with $\nu = a\tilde{\nu}$. As a conclusion, Theorem 3 is equivalent to a directional mixture representation. □

Remark Positive, finite directional mixtures of zonal anisotropies of variograms $\psi \in \Psi_d$ also define valid anisotropic variograms for a larger class of variograms than those verifying the conditions of Theorem 3. It is in particular the case for variograms whose principal irregular term are proportional to $r^2 \log r$ or proportional to r^2 as $r \to 0$.

4.3 Simulations of Anisotropic Fields

The above representation provides the basis for simulating anisotropic random fields, using an anisotropic version of the turning band simulation algorithm (Lantuéjoul 2002). The general idea is to reduce the simulation of Z to the simulations of N independent processes with variogram ψ. The expectation with respect to the measure $\tilde{\nu}$ in Eq. (7) is replaced by the arithmetic mean taken on the N independent realizations of $Z_{\eta_i}(\cdot)$, where $(\eta_i)_{i=1,\ldots,N}$ are independent directions drawn according to the probability distribution $\tilde{\nu}$. The pseudo-code for generating an anisotropic model is the following:

Algorithm `Simulate_Anistropic_Random_Field`

1. Set N
2. Compute $\nu_0 = \nu([0, 2\pi[)$
3. For $i = 1, \ldots, N$
   (a) Draw a random direction $\eta_i \sim \tilde{\nu} = \nu/\nu_0$
   (b) On the real line simulate a Gaussian process $Y_i(\cdot)$ with variogram $\psi \in \Psi_d$.
4. For all sites $s_j = (r_j, \theta_j)$, $j = 1, \ldots, n$ on which the simulation is to be performed, compute

$$Z(s_j) = \frac{1}{\sqrt{N}} \sum_{i=1}^{N} Y_i \left(r_j \nu_0^{1/\beta} \cos(\theta_j - \eta_i) \right).$$

5. Return $(Z(s_1), \ldots, Z(s_n))$.

Variograms ψ and γ are related by Eq. (7). Thanks to Theorem 3 the behavior at the origin of γ is the same as that of ψ, but the mixture representation changes the behavior of ψ away from the origin. Let us denote γ_{iso} an isotropic version of γ. Then, Eq. (7) can be re-written (Lantuéjoul 2002)

$$\gamma_{\text{iso}}(r) = 2\frac{(d-1)v_{d-1}}{dv_d} \int_0^1 \frac{\psi(tr)}{(1-t^2)^{(d-3)/2}} dt, \tag{9}$$

where v_d is the d-volume of the unit ball in $\mathbb{R}^d$.

When $d = 2$, Eq. (9) becomes $\gamma_{\text{iso}}(r) = \pi^{-1} \int_0^{\pi} \psi(r \sin u) du$ after the change of variable $t = \sin u$, thus leading to

$$\psi(r) = 1 + r \int_0^{\pi/2} \gamma'_{\text{iso}}(r \sin u) du, \tag{10}$$

where γ'_{iso} denotes the derivative of γ_{iso}. These formulas are still in integral form and not easily handled. Gneiting (1998) derives ψ explicitly for the most commonly used covariances. When $d = 3$, Eq. (9) reduces to

$$\gamma_{\text{iso}}(r) = \int_0^1 \psi(tr) dt, \quad \text{or} \quad \psi(r) = \gamma_{\text{iso}}(r) + r\gamma'_{\text{iso}}(r). \tag{11}$$

Remark 1. It is important to re-emphasize that contrarily to the usual turning band algorithm, the directions of the lines are not uniform but must be drawn according to the directional measure ν.
2. As apparent from Eqs. (10) and (11), the regularity at the origin is the same for ψ and γ. The mixture representation does not alter the regularity at the origin.
3. A similar idea has been recently proposed in Biermé, Moisan and Richard (2014) to simulate anisotropic fractional Brownian fields in two dimensions for a restricted class of anisotropy. Biermé, Moisan and Richard (2014) proposes a dynamic programming algorithm for optimizing the directions of the turning bands. Our implementation is thus slightly less efficient but much more general since the above algorithm is valid for any variogram, any dimension and all anisotropies.

5 Illustration: A Class of Anisotropy Models on the Plane

5.1 Classical Models of Anisotropy Revisited

In this section, it is illustrated how to use Theorem 4 in order to build anisotropic models. The case $d = 2$ will be retained for ease of exposition, but extension to higher dimensional spaces is straightforward, although cumbersome in terms of notation and difficult to represent. In $\mathbb{R}^2$, Eq. (6) simplifies to

$$b(\theta)^{-\beta} = \int_0^{2\pi} |\cos(\theta - \eta)|^{\beta} \nu(\mathrm{d}\eta). \tag{12}$$

Since ν is symmetric on $[0, 2\pi[$, the function $b(\cdot)$ is π-periodic, i.e. $b(\theta + \pi) = b(\theta)$. Moreover, if the measure ν is symmetric around a principal direction θ_0, so will be the function $b(\cdot)$. Specific cases of Eq. (12) correspond to the well known models of anisotropy reviewed in Sect. 3.

5.1.1 Isotropy

Obviously, if ν is rotationally invariant, that is if it is constant on $[0, 2\pi)$, the function $b(\theta)$ is also rotationally invariant and thus constant. The associated covariance is thus isotropic.

5.1.2 Zonal Anisotropy

When the measure ν in Eq. (6) is the sum of two Dirac measures in opposite directions

$$\nu(\mathrm{d}\eta) = 0.5 \left(b^{-\beta}\delta_{\theta_0} + b^{-\beta}\delta_{-\theta_0}\right)(\mathrm{d}\eta),$$

direct inspection shows that $b(\theta) = b/|\cos(\theta - \theta_0)|$ which corresponds to the zonal anisotropy model $\gamma(h) = \psi\{r|\cos(\theta - \theta_0)|/b\}$, with $\psi \in \Psi_2$.

5.1.3 Anisotropy Corresponding to Separable Covariances

This case is obtained by setting the measure ν as the sum of two Dirac measures in perpendicular directions

$$\nu(\mathrm{d}\eta) = 0.5\left(b_1^{-\beta}\delta_{\theta_0} + b_1^{-\beta}\delta_{\pi+\theta_0}\right)(\mathrm{d}\eta) + 0.5\left(b_2^{-\beta}\delta_{\theta_0+\pi/2} + b_2^{-\beta}\delta_{\theta_0+3\pi/2}\right)(\mathrm{d}\eta).$$

Direct inspection shows that

$$b(\theta) = \left\{|\cos(\theta-\theta_0)/b_1|^\beta + |\sin(\theta-\theta_0)/b_2|^\beta\right\}^{-1}, \tag{13}$$

which corresponds to separable covariance functions, that is covariance functions that are the product of two covariances defined on the real line, along the directions θ_0 and $\theta_0 + \pi/2$, that is $\gamma(h) = 1 - \{1 - \psi(|h_1|/b_1)\}\{1 - \psi(|h_2|/b_2)\}$, where $h_1 = r\cos(\theta-\theta_0)$ and $h_2 = r\sin(\theta-\theta_0)$, and $\psi \in \Psi_2$. The first row of Fig. 2 shows in a polar representation the scale parameter $b(\theta)$ as a function of θ for different values of β. Let $g(r) = r^\beta$ be the principal irregular term of ψ. Then, direct inspection shows that the principal irregular term of γ in the direction θ is

$$\begin{aligned} g_\theta(r) &= 1 - \left[1 - r^\beta\{|\cos(\theta-\theta_0)|/b_1\}^\beta\right]\left[1 - r^\beta\{|\sin(\theta-\theta_0)|/b_2\}^\beta\right] \\ &= r^\beta\{\cos(\theta-\theta_0)|/b_1\}^\beta + r^\beta\{|\sin(\theta-\theta_0)|/b_2\}^\beta \end{aligned}$$

which shows clearly that the principal irregular term arising from separable covariances is similar to that arising from the sum of zonal anisotropies in perpendicular directions.

5.1.4 Geometric Anisotropy

The geometric anisotropy corresponds to

$$\gamma(h) = \psi\left(\|Ah\|\right) = \psi\left(r\left[\{\cos(\theta-\theta_0)/b_1\}^2 + \{\sin(\theta-\theta_0)/b_2\}^2\right]^{1/2}\right),$$

where $\psi \in \Psi_2$. Then, Eq. (12) becomes

$$b(\theta)^{-\beta} = \{[\cos(\theta-\theta_0)/b_1]^2 + [\sin(\theta-\theta_0)/b_2]^2\}^{\beta/2} = \int_0^{2\pi} |\cos(\theta-\eta)|^\beta \nu(\mathrm{d}\eta). \tag{14}$$

This equation is a special instance of a Fredholm integral equation of the first kind. It is easily solved when $\beta = 2$. In this case, a simple solution is the sum of Dirac measures in the directions θ_0 and $\theta_0 + \pi/2$

$$\nu(\mathrm{d}\eta) = 0.5\left[b_1^{-2}\delta_{\theta_0} + b_1^{-2}\delta_{\pi+\theta_0}\right](\mathrm{d}\eta) + 0.5\left[b_2^{-2}\delta_{\theta_0+\pi/2} + b_2^{-2}\delta_{\theta_0+3\pi/2}\right](\mathrm{d}\eta),$$

which is nothing but the anisotropy corresponding to separable covariance functions seen above with $\beta = 2$. Finding exact solutions in the general case $0 < \beta < 2$

is a task which would lead us beyond the scope of this paper, this section being meant to be illustrative. Excellent approximate solutions will be shown in the next section.

5.2 A New Class of Anisotropy Models

5.2.1 General Construction

The directional mixture representation in Eq. (12) opens new avenues for building a large variety of valid anisotropic models. Anisotropy models are defined by the directional measure ν, which the modeling as a sum of kernels, wrapped on the circle, is proposed. Let us consider an even kernel function $k(\cdot)$ of unit mass, and let us denote $k_{h,x_0}(x) = h^{-1}k\{(x - x_0)/h\}$, with $h > 0$ and $x \in \mathbb{R}$. Since ν must be π-periodic, anisotropy models will thus be defined as the weighted sum of $2J$ kernels characterized by directions θ_j and windows h_j

$$\nu(\mathrm{d}\eta) = \sum_{j=1}^{J} 0.5 \left\{ c_j^{-\beta} k_{h_j,\theta_j}(\eta) + c_j^{-\beta} k_{h_j,\theta_j+\pi}(\eta) \right\} \mathrm{d}\eta. \tag{15}$$

Each kernel is weighted by factor $c_j^{-\beta}$, so that the values c_j can be interpreted as scale factors in the direction θ_j. Specific examples with Gaussian, squared cosine and bi-squared kernels will be shown later. This class includes zonal anisotropies as well as anisotropies arising from separable models by letting $k_{h_j,\theta_j} \to \delta_{\theta_j}$ when $h_j \to 0$.

5.2.2 Two Perpendicular Directions

To illustrate this class of models, first consider anisotropy models obtained when considering two similar kernels in perpendicular directions θ_0 and $\theta_0 + \pi/2$, with identical window parameter h

$$\begin{aligned} \nu(\mathrm{d}\eta) = {} & 0.5c_1^{-\beta}\{k_{h,\theta_0}(\eta) + k_{h,\theta_0+\pi}(\eta)\}\mathrm{d}\eta \\ & + 0.5c_2^{-\beta}\{k_{h,\theta_0+\pi/2}(\eta) + k_{h,\theta_0+3\pi/2}(\eta)\}\mathrm{d}\eta. \end{aligned} \tag{16}$$

Figures 2 and 3 show a polar representation of the scale parameter $b(\theta)$. These plots demonstrate clearly that it is possible to obtain, for a fixed value of β, a much larger variety of graphs than those summarized in Table 2. When $\beta \geq 1$, Eq. (12) implies that the graph of $b(\theta)$ as a function θ describes the boundary of a symmetric, closed, and convex set (see panels in the middle and right columns), tending to an ellipse as $\beta \to 2$. On the contrary, the graph is non convex when $\beta < 1$, with an increasing convexity as h increases. When $c_1 = c_2$, and $k_{h,\theta_0} = k_{h,\theta_0+\pi/2}$ the periodicity of $b(\theta)$ is equal to $\pi/2$, as in Fig. 2. When one of these two conditions is not verified, the periodicity of $b(\theta)$ is equal to π. Figure 3 illustrates some anisotropy models when $c_2 \neq c_1$ and $k_{h,\theta_0} = k_{h,\theta_0+\pi/2}$. As $h \to \infty$, we get that $\nu(\mathrm{d}\eta) \to \nu_\infty$ for all η, which means that the model tends to an isotropic model.

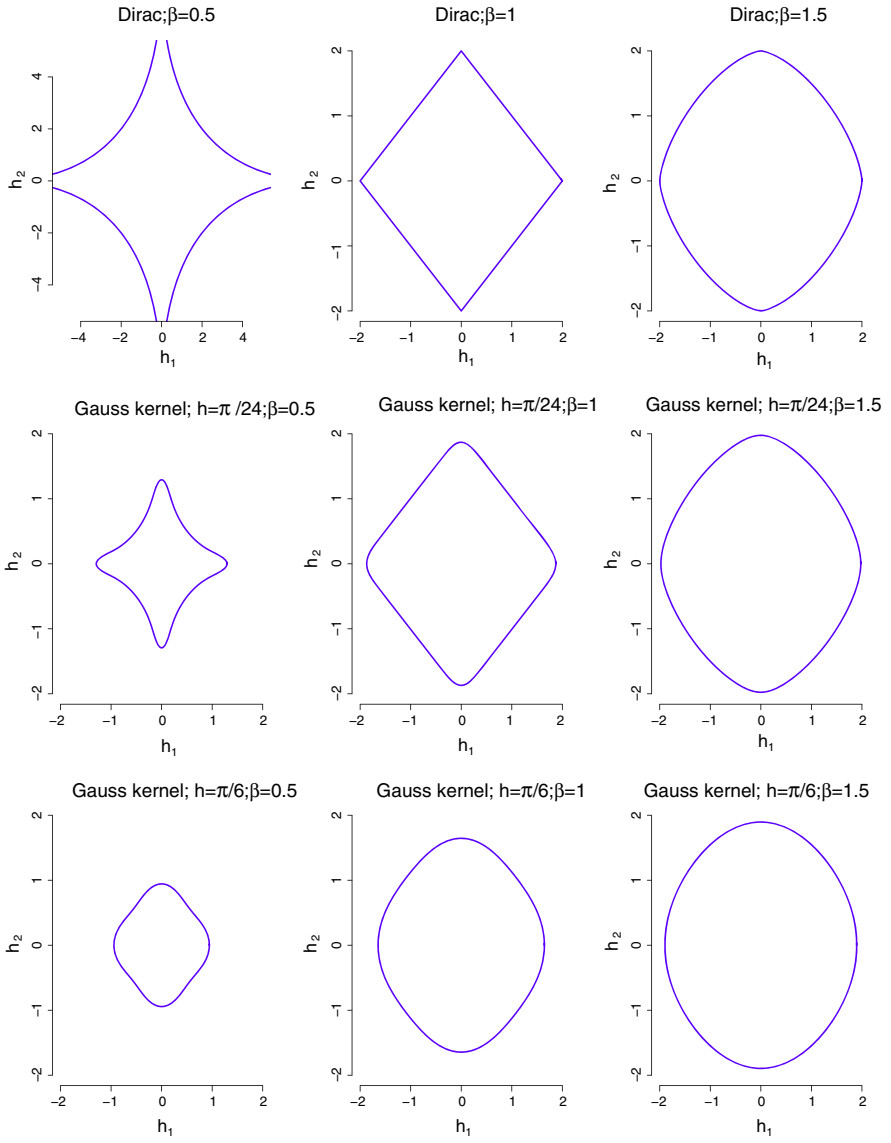

Fig. 2 Anisotropy models corresponding to the sum of two kernels, as in Eq. (16). *Top row* sum of two Dirac measures (corresponding to separable models of covariance). *Middle row* sum of two Gaussian kernels with $h = \pi/24$. *Bottom row* same with $h = \pi/6$. From *left* to *right* $\beta = 0.5, 1, 1.5$. For all models, $\theta_0 = 0$, $c_1 = c_2 = 2$

Figure 4 shows two realizations of Gaussian random fields with an anisotropy models corresponding to Eq. (16), for both an exponential covariance function and a power variogram with $\beta = 1.2$. Simulations were performed using the `R` package `RandomFields` (Schlather et al. 2015) according the algorithm `Simulate_Anistropic_Random_Field` presented in Sect. 4.3. These realiza-

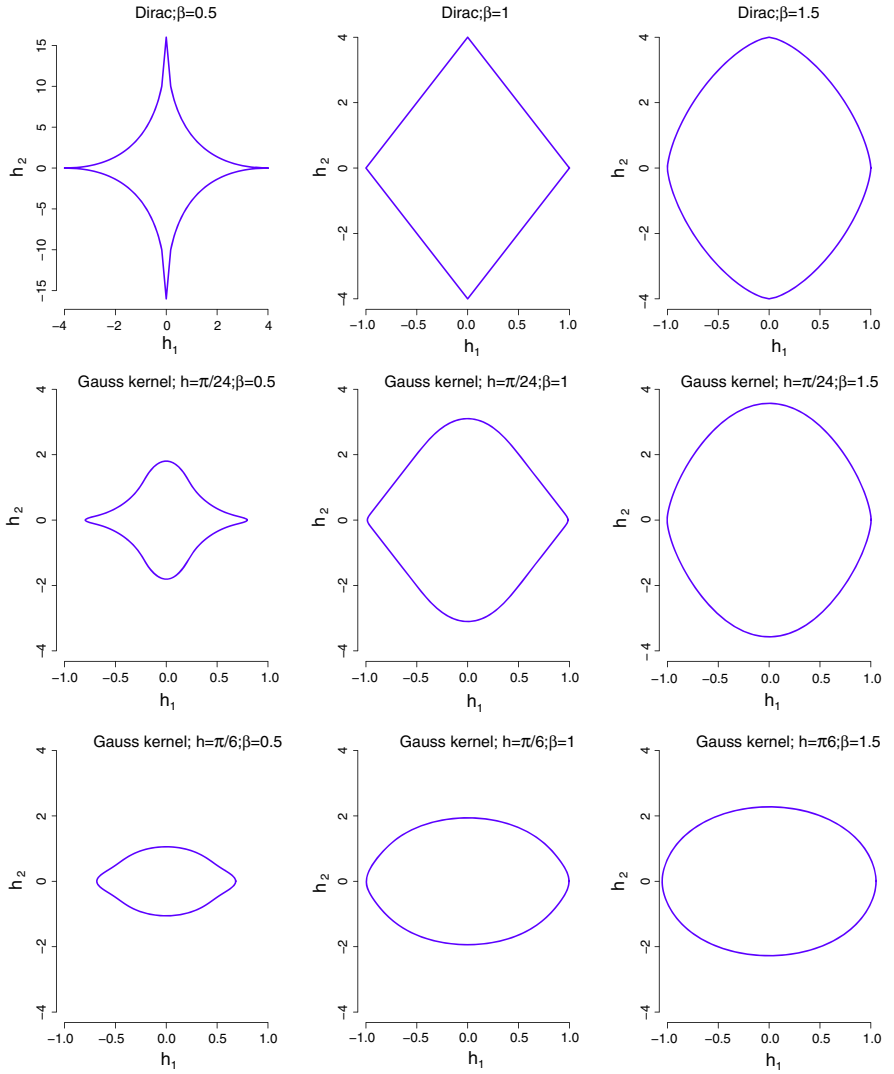

Fig. 3 Anisotropy models corresponding to the sum of two kernels. Same as Fig. 2, but here $c_1 = 1$ and $c_2 = 4$

tions show clearly anisotropic patterns that are very different to those obtained with geometric or separable anisotropies (not shown here). In contrast to patterns arising from separable covariances, there is some amount of variability around the two main anisotropy directions.

5.2.3 Geometric Anisotropy

Excellent approximate solutions to geometric anisotropies can be obtained using the following sum of kernels in perpendicular directions

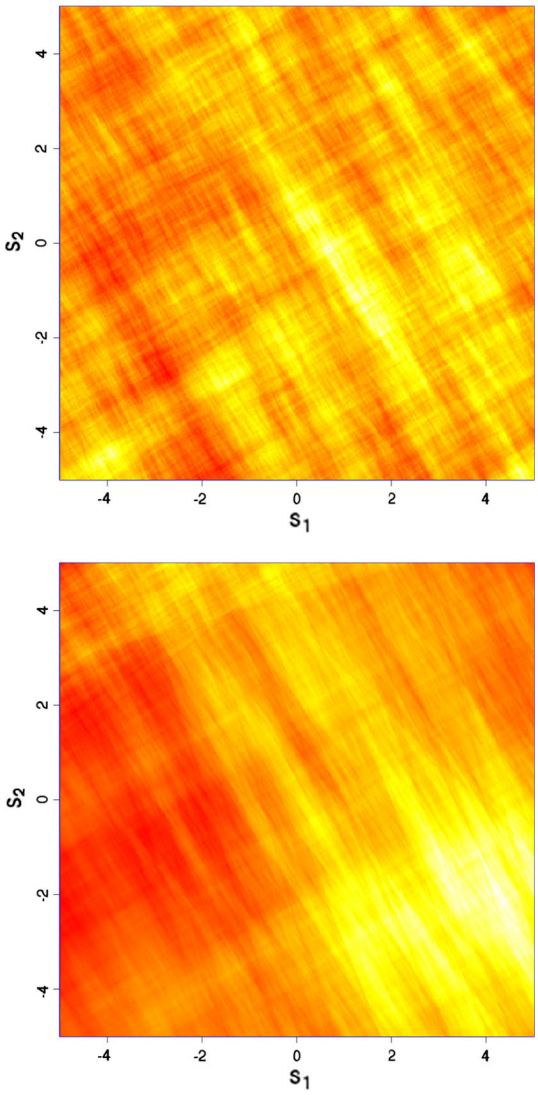

Fig. 4 Realizations of Gaussian random fields with an anisotropy model with two squared cosine kernels as in Eq. (16), with $c_1 = 1$, $c_2 = 2$, $h = \pi/8$ and $\theta_0 = \pi/6$. *Top* exponential covariance function. *Bottom* power variogram with power $\beta = 1.2$

$$\nu(\mathrm{d}\eta) = \left[\frac{b_1^{-\beta} + b_2^{-\beta}}{2} + \frac{b_1^{-\beta} - b_2^{-\beta}}{2\widehat{k}(2h)}\right]^{2/\beta} k_{h,\theta_0}(\eta)\mathrm{d}\eta + \left[\frac{b_1^{-\beta} + b_2^{\beta}}{2} - \frac{b_1^{-\beta} - b_2^{-\beta}}{2\widehat{k}(2h)}\right]^{2/\beta} k_{h,\theta_0+\pi/2}(\eta)\mathrm{d}\eta, \tag{17}$$

where $\widehat{k}(\omega)$ is the Fourier transform of the kernel function $k(\eta)$. The coefficients multiplying the kernel functions correspond to the exact geometric anisotropy model

Table 3 Some usual kernels and their corresponding Fourier transform

Name	Kernel, $k(x)$	Fourier transform, $\hat{k}(\omega)$
Gaussian	$\pi^{-1/2}\exp(-x^2)$	$\exp(-\omega^2/4)$
Squared cosine	$\cos^2(x\pi/2)\mathbf{1}_{(-1,1)}$	$\{\sin(\pi-\omega)+2\sin(\omega)+\sin(\pi+\omega)\}/2$
Bi-squared	$15/16(1-x^2)^2\mathbf{1}_{(-1,1)}$	$-15\{(\omega^2-3)\sin\omega+3\omega\cos\omega\}/\omega^5$

For each kernel, $k(x)$, its Fourier transform is $\hat{k}(\omega)$. All kernels have been standardized such that $\int_{\mathbb{R}} k(x)dx = 1$. The function $\mathrm{sinc}(x)$ is the sine cardinal function: $\mathrm{sinc}(x) = \sin(x)/x$

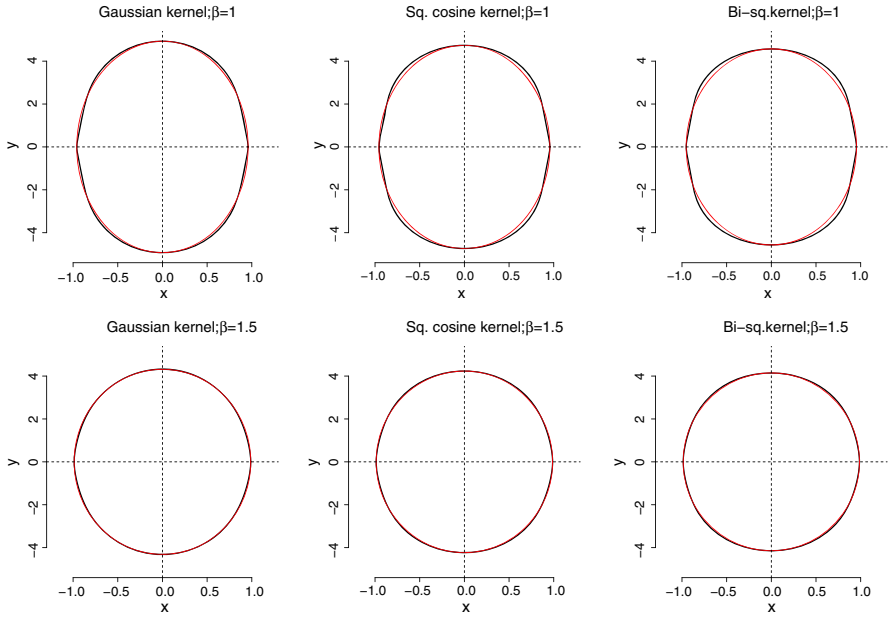

Fig. 5 *Black line* scale parameter $b(\theta)$ as a function of the angle, for models of anisotropies as defined in Eq. (17), with $c_1 = 1$ and $c_2 = 4$. From *left* to *right* Gaussian kernel with $h = \pi/12$; squared cosine kernel with $h = \pi/6$; bi-squared kernel with $h = \pi/6$. *Red solid line* geometric anisotropy with same range for $\theta \in \{0, \pi/2\}$. *Top row* $\beta = 1$; *bottom row* $\beta = 1.5$

with scale factors equal to b_1 and b_2 along directions θ_0 and $\theta_0 + \pi/2$ when $\beta = 2$. Table 3 provides the correspondence between the Gaussian, squared cosine and bi-squared kernels and their respective Fourier transform value $\widehat{k}(\omega)$.

Figure 5 represents on a polar graph the scale factor $b(\theta)$ resulting from this approximation. The corresponding geometrically anisotropic models are also represented. It can be observed that the match is excellent, well within statistical fluctuations usually observed on data. As expected the approximation is better for larger values of β in agreement with the fact that geometric anisotropy is exactly recovered when $\beta \to 2$. There are only slight differences from one kernel to the other. On all tested situations, it was found that the choice of the kernel is secondary as compared to the choice the bandwidth.

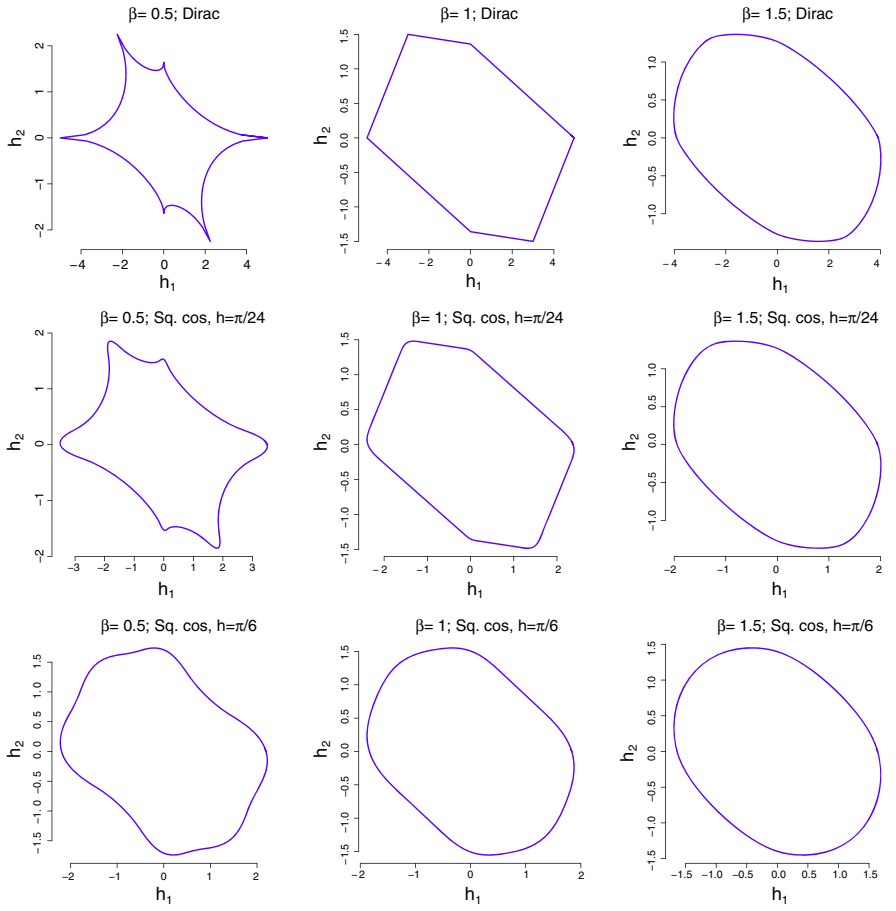

Fig. 6 Anisotropy models corresponding to the sum of three kernels, as in Eq. (13). *Top row* sum of Dirac measures. *Middle row* sum of squared cosine kernels with $h = \pi/24$. *Bottom row* same with $h = \pi/6$. From *left* to *right* $\beta = 0.5, 1, 1.5$. For all models, $(c_1, c_2, c_3) = (1, 2, 3)$

5.2.4 Three Directions

This class of anisotropies is not limited to the sum of two kernels located at θ_0 and $\theta_0 + \pi/2$. In sharp contrast with usual models, anisotropies with more than two principal directions can easily be defined. Figure 6 shows some anisotropic models obtained when considering three components in Eq. (15). Figure 7 shows two realizations of Gaussian random fields with a spherical covariance model and with a linear variogram. The anisotropy model is the result of the sum of three kernels along $(\theta_1, \theta_2, \theta_3) = (0, \pi/6, \pi/3)$. The three main directions are clearly visible, in particular in the stationary case. The simulated pattern is very different to any pattern obtained with usual anisotropy models.

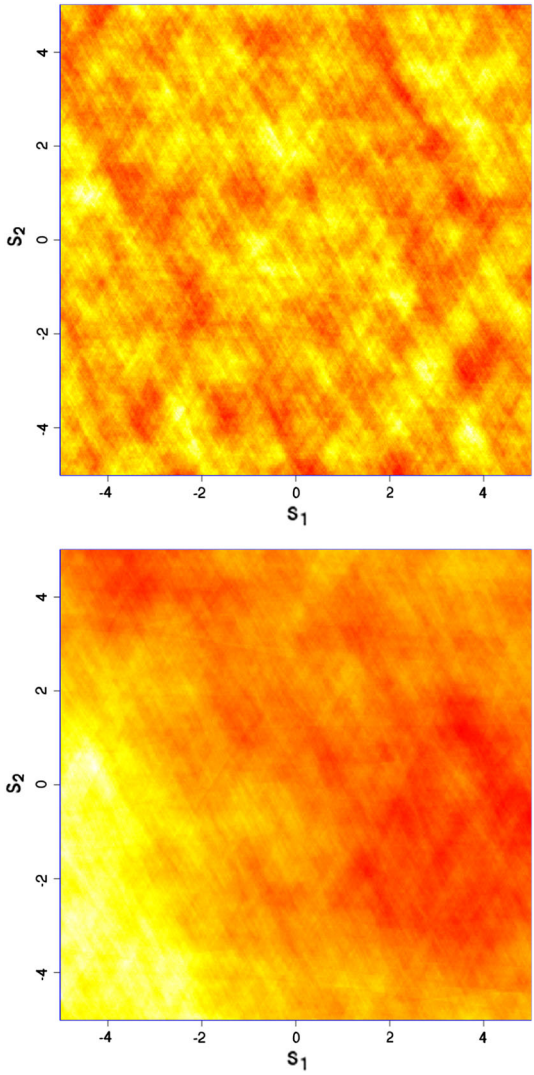

Fig. 7 Realizations of Gaussian random fields with an anisotropy models with three squared cosine kernels, with $(\theta_1, \theta_2, \theta_3) = (0, \pi/6, \pi/3)$, $(c_1, c_2, c_3) = (1, 2, 3)$ and $h = \pi/6$. *Top* spherical covariance function. *Bottom* power variogram with $\beta = 1$

6 Conclusion and Discussion

In this paper strategies allowing to go beyond classical anisotropies were explored. It was first proved that if the regularity parameter of a variogram does not vary discontinuously with the direction, it must necessarily be constant. Then, a necessary and sufficient characterization of the anisotropy of the scale parameter as directional mixtures of zonal anisotropy variograms is provided. From this characterization, a straightforward simulation algorithm is derived. Far beyond the classic zonal or geometric models of anisotropy, this representation offers a great variety of anisotropy models. As a practical way to model anisotropies in this context, a semi-parametric

class of of the directional mixture, defined as the weighted sum of kernel functions located at J main directions $(\theta_j)_{j=1,\ldots,J}$, has been proposed.

The findings reported in this work open new avenues for the modeling of anisotropic random fields. This paper must be seen as a first theoretical step in that direction. Further work is required in various directions in order build a practical geostatistical modeling strategy. The mixture representation offers two approaches to estimate a valid anisotropy model as given in Theorem 4. Ongoing research is undertaken to estimate the parameters of the semi parametric model proposed in Eq. (15) using the weighted composite likelihood proposed in Bevilacqua et al. (2012). Other semi-parametric models and/or competing estimation procedures could be proposed. In particular, the promising Bayesian approach in Kazianka (2013) could be generalized to our representation. Alternatively, the mixture measure can be estimated non parametrically by estimating the scale parameter $b(\theta)$ in various directions and inverting Eq. (8). This work holds the potential to initiate further theoretical work. Two possible research directions are highlighted. Firstly, relationships with space-time covariance modeling should be systematically explored, in particular in the light of the recent developments in Stein (2013), where generalized covariance with different smoothness parameters in space and time were proposed within the framework of Intrinsic Random Functions of order k. Secondly, extensions to processes defined over the sphere, for which the Euclidean distance is no longer a suitable metric, would be of great interest for model global processes on the planet Earth.

Appendix A: Proofs

Proof of Proposition 1

The "only if" part is proven by building a simple counter-example in $\mathbb{R}^2$. Let (r, θ) be the polar coordinates of h. Since $\beta(\theta)$ is a continuous function of θ on a compact set, there exists β_1 such that $0 < \beta_1 = \min_\theta\{\beta(\theta)\} \leq \beta(\theta)$. Without loss of generality, the X-axis is a (non necessarily unique) direction for which $\beta(\theta)$ is minimum, i.e. $\beta(0) = \beta_1$. Recall that $\beta(\theta) = \beta(\theta + \pi)$ because the variogram is an even function. Let us consider the points $s_0 = (0, 0)$, $s_1 = (-x, y)$ and $s_2 = (x, y)$, with $x, y > 0$. The contrast

$$Z(0,0) - Z(-x,y)/2 - Z(x,y)/2 = \sum_{i=0}^{2} w_i Z(s_i),$$

corresponds to the error made when predicting the value at s_0 with the average of the values located at s_1 and s_2. Let us examine the sign of the quadratic form

$$\begin{aligned} Q &= -\sum_{i=0}^{2}\sum_{j=0}^{2} w_i w_j \gamma(s_i - s_j) \\ &= \gamma_{\mathrm{AP}}\{(-x,y)\} + \gamma_{\mathrm{AP}}\{(x,y)\} - 0.5\gamma_{\mathrm{AP}}\{(2x,0)\} \\ &= a(\pi-\theta)r^{\beta(\pi-\theta)} + a(\theta)r^{\beta(\theta)} - 0.5a(0)(2x)^{\beta_1}, \end{aligned}$$

where θ denotes the angle of the vector $s_2 - s_0$ with the X-axis and $r^2 = x^2 + y^2$. The quadratic form Q would correspond to the variance of the linear combination if $\gamma_{\mathrm{AP}}(h)$ was a valid variogram. Let us denote $\beta_m = \min\{\beta(\pi - \theta), \beta(\theta)\} \geq \beta_1$. Using $x = r\cos\theta$ and dividing by r^{β_m} the above expression becomes

$$\frac{Q}{r^{\beta_m}} = a(\pi - \theta)r^{\beta(\pi-\theta)-\beta_m} + a(\theta)r^{\beta(\theta)-\beta_m} - 0.5a(0)(2r\cos\theta)^{\beta_1-\beta_m}. \quad (18)$$

As $r \to 0$, the first two terms in (18) are bounded by $a(\pi - \theta) + a(\theta)$ and the last term is proportional to $-r^{\beta_1-\beta_m}$ with $\beta_1 \leq \beta_m$. Hence, Q becomes negative as $r \to 0$ unless $\beta_m = \beta_1$. Hence, for all $0 < \theta < \pi/2$

$$Q \geq 0 \text{ as } x \to 0 \Leftrightarrow \min_{\theta}\{\beta(\pi - \theta), \beta(\theta)\} = \beta_1. \quad (19)$$

Using topological arguments, one can then show that $\beta(\theta) = \beta_1$, for all θ. The proof is completed by noticing that if a function is not c.d.n. in $\mathbb{R}^2$, it is not c.d.n. in $\mathbb{R}^d$, for $d \geq 2$. □

Proof of Theorem 2

For the same construction as in Proposition 1, the quadratic form Q now reads

$$Q = a(\pi - \theta)r^{\beta(\pi-\theta)}f(r) + a(\theta)r^{\beta(\theta)}f(r) - 0.5a(\theta)(2x)^{\beta_1}f(2x),$$

and thus

$$\frac{Q}{f(r)r^{\beta_m}} = a(\pi - \theta)r^{\beta(\pi-\theta)-\beta_m} + a(\theta)r^{\beta(\theta)-\beta_m} - 0.5a(0)(2\cos\theta)^{\beta_1-\beta_m}\frac{f(2r\cos\theta)}{f(r)}r^{\beta_1-\beta_m}. \quad (20)$$

As $r \to 0$, the first two terms in (20) are bounded and, since f is a slowly varying function at $r = 0$, the last term tends to $-\infty$. Hence, Q becomes negative as $r \to 0$ unless $\beta_m = \beta_1$. The end of the proof is now exactly similar to that of Proposition 1. □

References

Bevilacqua M, Gaetan C, Mateu J, Porcu E (2012) Estimating space and space-time covariance functions for large data sets: a weighted composite likelihood approach. J Am Stat Assoc 107:268–280

Biermé H, Moisan L, Richard F (2014) A turning-band method for the simulation of anisotropic fractional Brownian fields. J Comput Graph Stat. doi:10.1080/10618600.2014.946603

Chiles JP, Delfiner P (2012) Geostatistics: modeling spatial uncertainty, 2nd edn. John Wiley & Sons, New-York

Daley DJ, Porcu E (2014) Dimension walks through Schoenberg spectral measures. Proc Am Math Soc 142:1813–1824

Davies S, Hall P (1999) Fractal analysis of surface roughness by using spatial data. J R Stat Soc B 61:3–37

Dowd A, Igúzquiza E (2012) Geostatistical analysis of rainfall in the West African Sahel. In: Gómez-Hernández J (ed) IX Conference on Geostatistics for Environmental Applications, geoENV2012, Editorial Universitat Politècnica de València, pp 95–108
Eriksson M, Siska P (2000) Understanding anisotropy computations. Math Geol 32:683–700
Gneiting T (1998) Closed form solutions of the two-dimensional turning bands equation. Math Geol 30: 379–390
Gneiting T, Sasvari Z, Schlather M (2001) Analogies and correspondences between variograms and covariance functions. Adv Appl Probab 33:617–630
Journel A, Froidevaux R (1982) Anisotropic hole-effect modeling. Math Geol 14:217–239
Kazianka H (2013) Objective bayesian analysis of geometrically anisotropic spatial data. J Agric Biol Environ Stat 18:514–537
Ma C (2007) Why is isotropy so prevalent in spatial statistics? Trans Am Math Soc 135:865–871
Lantuéjoul C (2002) Geostatistical simulation. Models and algorithms. Springer, Berlin
Matheron G (1970) La théorie des variables régionalisées et ses applications. Cahiers du Centre de Morphologie Mathématique de Fontainebleau, Fasc. 5, Ecole des Mines de Paris. Translation (1971): The Theory of Regionalized Variables and Its Applications
Matheron G (1975) Random sets and integral geometry. John Wiley & Sons, New York
Porcu E, Schilling R (2011) From Schoenberg to Pick-Nevanlinna: toward a complete picture of the variogram class. Bernoulli 17:441–455
Porcu E, Gregori P, Mateu J (2006) Nonseparable stationary anisotropic space-time covariance functions. Stoch Environ Res Risk Assess 21:113–122
Schlather M et al (2015) Package 'RandomFields'. http://cran.r-project.org/web/packages/RandomFields/
Stein M (1999) Interpolation of spatial data: some theory for kriging. Springer, New-York
Stein M (2013) On a class of space-time intrinsic random functions. Bernoulli 19:387–408
Schoenberg IJ (1938) Metric spaces and positive definite functions. Trans Am Math Soc 44:522–536